Large reversible magnetocaloric effect in $HoMn_2O_5$*

Ge Heng(葛 恒)[a)b)], Zhang Xiang-Qun(张向群)[b)], Ke Ya-Jiao(柯亚娇)[b)], Jin Jin-Ling(靳金玲)[b)], Liao Zhi-Xin(廖志新)[a)], and Cheng Zhao-Hua(成昭华)[b)†]

[a)] *School of Chemistry and Chemical Engineering, Southeast University, Nanjing* 210009, *China*
[b)] *State Key Laboratory of Magnetism, Institute of Physics, Chinese Academy of Sciences, Beijing* 100190, *China*

(Received 25 November 2012; revised manuscript received 10 January 2013)

Magnetocaloric effect (MCE) in polycrystalline $HoMn_2O_5$ was investigated by isothermal magnetization curves from 2 K to 50 K. A relatively large magnetic entropy change, $\Delta S_M = 7.8$ J/(kg·K), was achieved with the magnetic field up to 70 kOe (1 Oe = 79.5775 A·m^{-1}). The magnetic entropy change is reversible in the whole range of temperature. The contributions of elastic and magnetoelastic energy to the changing of the magnetic entropy are discussed in terms of the Landau theory. The reversibility of MCE with maximal refrigerant capacity $R_C = 216.7$ J/kg makes polycrystalline $HoMn_2O_5$ promising as a magnetic refrigerant.

Keywords: $HoMn_2O_5$, magnetocaloric effect

PACS: 75.47.Lx, 75.30.Sg **DOI:** 10.1088/1674-1056/22/5/057502

1. Introduction

Magnetic refrigeration, based on the magnetocaloric effect (MCE), has attracted wide interest because of its high energy efficiency and environment-friendliness. It is meaningful to explore prominent refrigerants for different working temperature ranges with larger entropy change and little hysteresis of both the temperature and the magnetic field. RMn_2O_5 (R represents the rare earth element) is orthorhombic, has *Pbam* space group symmetry,[1] and it contains infinite chains of $Mn^{4+}O_6$ octahedra sharing edges, linked together by $Mn^{3+}O_5$ and HoO_8 units.[2,3] The characteristic magnetic ordering of the system exhibits a transition from incommensurate to commensurate, and then to incommensurate antiferromagnetic (AFM) magnetic structure with the decrease of the temperature.[4] For example, the past reports indicated that $HoMn_2O_5$ displays a series of complicated phase transitions due to both the long range ordering of Ho^{3+} moments and the coexistence of Mn^{3+} and Mn^{4+}. Long-range AFM ordering of the Mn^{3+}/Mn^{4+} spins occurs at the temperature of $T_N = 43$ K. Subsequently, the ferroelectric (FE) transition takes place at the temperature of T_C= 39 K, slightly below T_N. Another magnetic transition occurs at the temperature of $T'_N = 22.5$ K, when commensurate AFM ordering becomes incommensurate. Below 19 K, the phase transition from incommensurate AFM ordering to canted AFM takes place and a second CAFM-type ordering of the Ho ions occurs at T_N(Ho) below 10 K.[5–7] As a result, this type of manganese oxide shows many interesting physical characteristics in dielectric properties, special heat, and thermal expansion behaviors.[8–11] In addition, RMn_2O_5 has attracted wide interests as a multiferroic material. Its magnetostriction effect[12,13] and the magnetoelectric coupling effect[14–18] have been studied extensively. The external magnetic field can induce and/or modify the ferroelectric states in RMn_2O_5 (R = Dy, Ho, etc.).

Its magnetostriction effect,[12,13] especially the magnetoelectric coupling effect,[14–18] in which an external magnetic field induces and/or modifies the ferroelectric states in RMn_2O_5 (R = Dy, Ho, etc), has been studied extensively.

Under an external magnetic field, the complicated magnetic structure results in complicated magnetic phases. Although the giant anisotropy of the magnetocaloric effect has been studied in $RMnO_3$ single crystals[19,20] with various spiral magnetic structures, the effect of the complicated magnetic structure in RMn_2O_5 on its MCE is not yet well understood. In this paper, we focus on the MCE in a polycrystalline $HoMn_2O_5$ sample.

2. Experiment

The polycrystalline, single-phase sample $HoMn_2O_5$ was synthesized through a standard solid-state reaction method. Stoichiometric amounts of Ho_2O_3 (99.95%), MnO_2 (99.9%) were thoroughly mixed, compressed into pellets, and then sintered at the temperature of 1120 °C for 48 h in O_2 atmosphere. The sample was finally cooled down to room temperature. X-ray powder diffraction (XRD) patterns were collected with Cu Kα radiation in a Rigaku RINT 1400. The XRD patterns proved that the sample was in pure phase with a polycrystalline structure. The results were analyzed by Rietveld method with the Rietica program. Magnetization measurements were carried out at a temperature ranging from 2 K to 300 K and mag-

*Project supported by the National Basic Research Program of China (Grant Nos. 2010CB934202 and 2011CB921801) and the National Natural Science Foundation of China (Grant Nos. 11174351 and 11274360).

†Corresponding author. E-mail: zhcheng@iphy.ac.cn

© 2013 Chinese Physical Society and IOP Publishing Ltd

netic field up to 70 kOe with a commercial superconducting quantum interference device (SQUID) magnetometer (Quantum design, MPMS-XL).

3. Results and discussion

Figure 1 shows the X-ray diffraction (XRD) patterns of $HoMn_2O_5$ at room temperature and the fitted results. The crosses and the red solid line represent the observed data points and the Rietveld refinement patterns, respectively. The vertical marks show the positions of Bragg diffraction. The green line means the difference between the observed and calculated intensities. The XRD patterns suggest that the sample is in pure phase with *Pbam* symmetry. The lattice parameters, $a = 7.2723$ Å, $b = 8.4682$ Å, and $c = 5.6667$ Å, refined by the Rietica program, are almost consistent with the reported values, $a = 7.2643(3)$ Å, $b = 8.4768(3)$ Å, and $c = 5.6700(2)$ Å.[1]

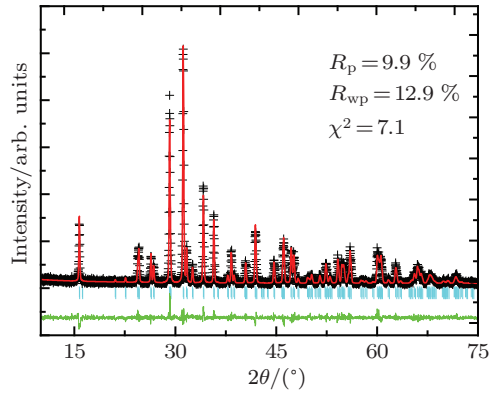


Fig. 1. (color online) XRD patterns of $HoMn_2O_5$ at room temperature and fitted results.

The thermal magnetization curves are shown in Fig. 2. The measurements are carried out under a magnetic field of 1 kOe after zero field cooling (ZFC) and field cooling (FC) processes, respectively. The magnetic transition is not obviously in the M–T curves, but it can be seen from $\partial M/\partial T$ that there is a kink point, corresponding to the antiferromagnetic ordering T_N(Ho), around 11 K. In addition, by fitting the experimental data points from 200 K to 300 K with the Curie–Weiss law, we obtain the Curie–Weiss temperature $\theta_p = -28$ K, which reflects the AFM interaction in the system. The effective magnetic moment $\mu_{eff} = 12.1\ \mu_B$, which is in good agreement with the theoretical effective $\mu_{cal} = 12.3\ \mu_B$ calculated by $\mu_{cal} = \sqrt{\mu_{eff}(Ho^{3+})^2 + \mu_{eff}(Mn^{3+})^2 + \mu_{eff}(Mn^{4+})^2}$.

Figure 3 presents the isothermal magnetization measured at different temperatures ranging from 2 K to 50 K, with an increment of 2 K, through increasing the magnetic field H from 0 kOe to 70 kOe and then decreasing to 0 kOe. The magnetization deceases gradually with the increase of the temperature. No visible phase transition can be detected from the magnetization curves. A complete reversibility of MCE requires that no hysteresis of either the temperature or the magnetic field appears in the vicinity of a magnetic ordering temperature.[21] There is almost no hysteresis of either temperature or magnetic field, as shown by the curves. The magnetic entropy change ΔS_M produced by the variation of external magnetic field from 0 to H can be calculated by[22]

$$\Delta S(T,H) = S(T,H) - S(T,0) = \int_0^H \left(\frac{\partial M}{\partial T}\right)_H \mathrm{d}H = \sum_0^H \left(\frac{M|_{T+\Delta T} - M|_{T-\Delta T}}{(T+\Delta T) - (T-\Delta T)}\right)_H \Delta H, \quad (1)$$

where $\Delta T = 1$ K and $\Delta H = 2$ kOe. The calculated $-\Delta S_M$ is shown as black dots in Fig. 4, and the peak of the magnetic entropy change appears below 17 K under different magnetic fields.

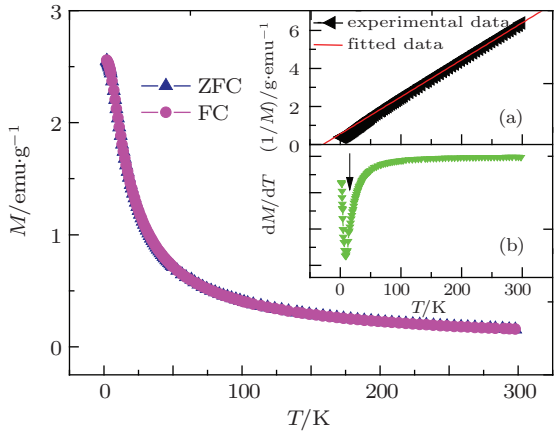


Fig. 2. (color online) Thermal magnetization curves of $HoMn_2O_5$ sample carried out under a magnetic field of 1 kOe after zero field cooling (ZFC) and field cooling (FC) processes. The inset (a) shows the relation of $1/M$ and the temperature T and the corresponding fitted curves with Curie–Weiss law, and inset (b) shows the $\partial M/\partial T$ as a function of temperature T. The black arrow points to the Ho^{3+} transition temperature.

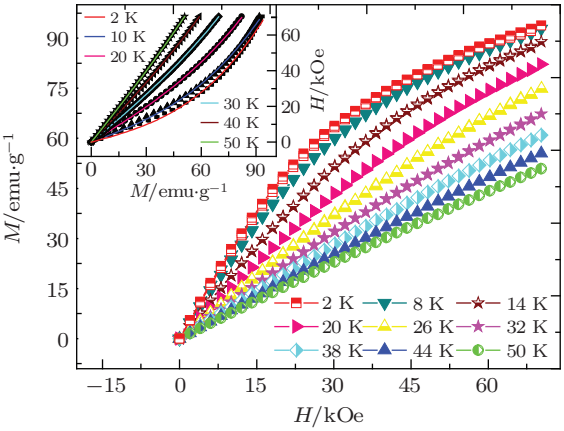


Fig. 3. (color online) Isothermal magnetization curves at different temperatures. The inset is the fitted results using Landau theory.

Refrigerant capacity (R_c) can be obtained by numerically integrating the area under the ΔS_M versus T curves, using the temperatures at half-maximum of the ΔS_M peak as the integration limits. Figure 5 demonstrates the values of R_C as a

function of the applied field. At 70 kOe, the refrigerant capability of the polycrystalline $HoMn_2O_5$ sample can be up to 216.7 J/kg.

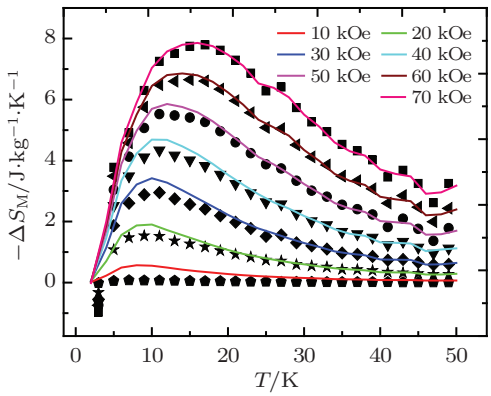


Fig. 4. (color online) Magnetic entropy change ΔS_M as a function of temperature in various magnetic fields. The black dots represent the ΔS_M calculated through Eq. (1) and solid lines correspond to the ΔS_M calculated through the Landau theory of phase transition, respectively.

In order to further understand the magnetic entropy change around the transition temperature of Ho^{3+}, we simulate it by Landau's theory of phase transition. Considering the symmetry, the Gibbs energy under an external magnetic field can be expressed as

$$G(T,H) = G_0 + A(T)M^2 + B(T)M^4 - MH, \tag{2}$$

where G_0 is the value for the highly symmetric state under zero magnetic field, and coefficients A and B can be expressed as functions of temperature. In addition, coefficient B is composed by elastic and magnetoelastic terms.[23] The condition $\partial G/\partial M = 0$ should be satisfied for an equilibrium state. Then, we can get the following equation:

$$H = 2A(T)M + 4B(T)M^3. \tag{3}$$

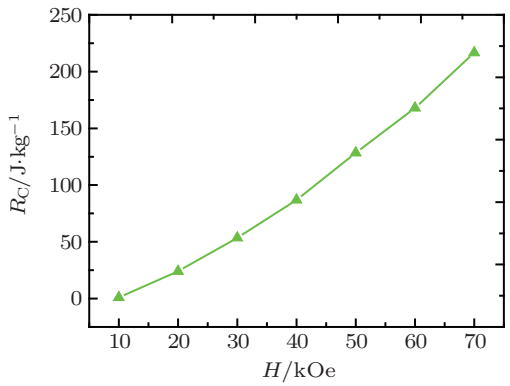


Fig. 5. (color online) Refrigeration capacity as a function of the external magnetic field.

By fitting the data in Fig. 3 according to Eq. (3), a fitted graph is obtained, as shown in the inset of Fig. 3.

The entropy as a function of temperature and magnetic field can be expressed as

$$S(T,H) = -\frac{\partial G(T,H)}{\partial T} = -\frac{\partial A(T)}{\partial T}M^2 - \frac{\partial B(T)}{\partial T}M^4. \tag{4}$$

The calculated magnetic entropy change under varied magnetic field is displayed in Fig. 4. The results are basically consistent with the values calculated through Eq. (1). Thus, the Landau theory of phase transition is enough to explain the change of the magnetic entropy.

Figure 6 presents the fitted values of coefficients A and B. With the increase of the temperature, A increases gradually, while B shows two anomalies at the temperature of 26 K and 42 K, which correspond exactly to the AFM transition T_N and another magnetic transition T_N'. Moreover, calculating the magnetic entropy change contribution of items A and B respectively, we find that the value of item A, corresponding to the changes of the magnetic moment structure in response to the magnetic field, is always negative. The maximum value of item A appears at the temperature of 16 K. The value of item B is positive below 26 K and then turns negative, and the maximally positive and negative values of item B are about 8 K and 40 K, respectively, which are very close to the phase transition temperatures T_N(Ho) around 10 K and $T_N = 43$ K.

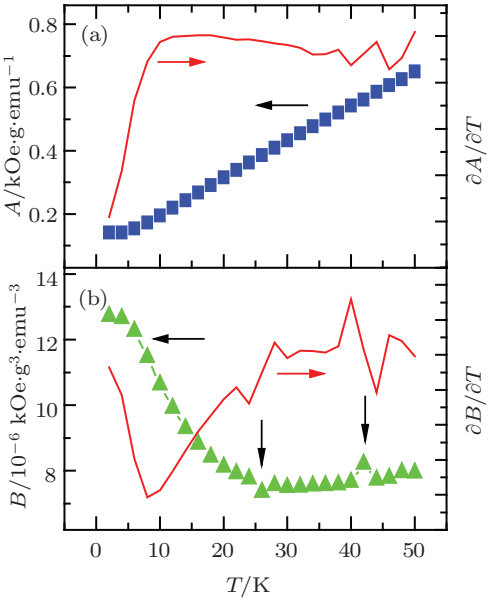


Fig. 6. (color online) (a) Fitted values of coefficients A and $\partial A/\partial T$, (b) coefficients B, and $\partial B/\partial T$ curves as a function of temperature. The arrows point to two anomalies in the curve $B(T)$ at 26 K and 42 K, corresponding to the magnetic transition at T_N' and T_N.

The colossal magnetostriction effect in $HoMn_2O_5$ monocrystals, resulting from a reorientation of the spin moments in an external magnetic field, has been observed.[24] From the above discussion in terms of Landau theory, the item A, corresponding to the changes of the structure of the magnetic moment in response to the magnetic field, contributes most of the magnetic entropy change. However, the contribution of both the elastic energy and magnetoelastic energy to the magnetic entropy change above 26 K is very small, which can be ignored. Considering the phase diagram composed by temperature and magnetic field,[12] the maximum

value of ΔS_M is shown in the region of a CAFM-type ordering (CAFM II) of the Ho ions, which means that as the temperature decreases, the ordering of Ho^{3+} moments, together with the rapid change of magnetization, respond mainly to the magnetic entropy change.

4. Summary

We investigated the MCE in a polycrystalline $HoMn_2O_5$ sample. Its refrigeration capacity is about 216.7 J/kg for the magnetic field up to 70 kOe. The main origin of the MCE in polycrystalline $HoMn_2O_5$ is the ordering of Ho^{3+} moments. In addition, the contribution of elastic energy and magnetoelastic energy to the change of magnetic entropy was discussed in terms of the Landau theory. The relative simplicity of the method and conditions for the preparation of $HoMn_2O_5$ polycrystalline makes it to be a meaningful candidate material for low-temperature refrigeration.

References

[1] Alonso J A, Casais M T, Martínez-Lope M J, Martínez J L and Fernández-Díaz M T 1997 *J. Phys.: Condens. Matter* **9** 8515

[2] Munoz A, Alonso J A, María T, Martínez-Lope M J , Martínez J L and Fernández-Díaz M T 2005 *Eur. J. Inorg. Chem.* 685

[3] Radaelli P G and Chapon L C 2008 *J. Phys.: Condens. Matter* **20** 434213

[4] Noda Y, Kimura H, Fukunaga M, Kobayashi S, Kagomiya I and Kohn K 2008 *J. Phys.: Condens. Matter* **20** 434206

[5] dela Cruz C R, Yen F, Lorenz B, Gospodinov M M, Chu C W, Ratcliff W, Lynn J W, Park S and Cheong S W 2006 *Phys. Rev. B* **73** 100406

[6] Chapon L C, Blake G R, Gutmann M J, Park S, Hur N, Radaelli P G and Cheong S W 2004 *Phys. Rev. Lett.* **93** 177402

[7] Radulov I, Nizhankovskii V I, Lovchinov V, Dimitrov D and Apostolov A 2006 *Eur. Phys. J. B* **52** 361

[8] Blake G R, Chapon L C, Radaelli P G, Park S, Hur N, Cheong S W and Rodríguez-Carvajal J 2005 *Phys. Rev. B* **71** 214402

[9] Hur N, Park S, Sharma P A, Guha S and Cheong S W 2004 *Phys. Rev. Lett.* **93** 107207

[10] Ratcliff W, Kiryukhin V, Kenzelmann M, Lee S H, Erwin R, Schefer J, Hur N, Park S and Cheong S W 2005 *Phys. Rev. B* **72** 060407

[11] Kobayashi S, Kimura H, Noda Y and Kohn K 2005 *J. Phys. Soc. Jpn.* **74** 468

[12] Fukunaga M, Kimura H, Noda Y and Kohn K 2007 *J. Korean Phys. Soc.* **51** 768

[13] Johnstone G E, Ewings R A, Johnson R D, Mazzoli C, Walker H C and Boothroyd A T 2012 *Phys. Rev. B* **85** 224403

[14] Hur N, Park S, Sharma P A, Ahn J S, Ahn J S, Guha S and Cheong S W 2004 *Nature* **429** 392

[15] Tyson T A, Deleon M, Yoong S and Cheong S W 2007 *Phys. Rev. B* **75** 174413

[16] Higashiyama D and Miyasaka S 2004 *Phys. Rev. B* **70** 174405

[17] Fukunaga M, Sakamoto Y, Kimura H, Noda Y, Abe N, Taniguchi K, Arima T, Wakimoto S, Takeda M, Kakurai K and Kohn K 2009 *Phys. Rev. Lett.* **103** 077204

[18] Higashiyama D and Miyasaka S 2005 *Phys. Rev. B* **72** 064421

[19] Midya A, Das S N and Mandal P 2011 *Phys. Rev. B* **84** 235127

[20] Jin J L, Zhang X Q, Ge H and Cheng Z H 2012 *Phys. Rev. B* **85** 214426

[21] Hu F X, Shen B G, Sun J R and Cheng Z H 2001 *Phys. Rev. B* **64** 012409

[22] Jin J L, Zhang X Q, Li G K and Cheng Z H 2011 *Phys. Rev. B* **83** 184431

[23] Lévy L P 2000 *Magnetism and Superconductivity* (Berlin: Springer)

[24] Radulov I, Lovchinov V, Dimitrov D and Apostolov A 2009 *J. Phys.: Conf. Ser.* **153** 012064